Evaluation of the shielding effectiveness of a multimode metallic cavity

D. CAZANARU, A. SZILAGYI, A. IOACHIM[b*]
Military Equipment & Technologies Research Agency, 16, Aeroportului, Clinceni, 077060, Bucuresti, Romania
[b]National Institute of Materials Physics, 105bis, Atomistilor, Magurele, 077125, Romania

Electronic equipment can be effectively shielded by the use of a conductive barrier placed between the source of electromagnetic waves and the equipment to be shielded. This paper describes a work which covers some considerations on the materials used for shielding and aspects of the design optimization from the electromagnetic compatibility point of view of a shield with application to a shielding box for a portable computer.

1. Introduction. Shielding effectiveness evaluation

In recent years the increasing use of the electronic equipment have led to complex electromagnetic interference (EMI) problems (called also electromagnetic pollution). This equipments typically generates electromagnetic energy that can interfere with the operation of other electronic equipment due to EMI transmission by radiation. Proper EMI control methodology and techniques are used to meet the electromagnetic compatibility (EMC) requirements.

Shielding is an essential part of an EMC design. Commonly, a shield is regarded as an enclosure from a suitable material, containing a number of circuits, power supplies and printed circuit boards. The shield can be considered, also, as the last obstacle to internally generated emissions before they are released into the external environment, and the first obstacle to external interference preventing it from reaching the internal circuits [1].

A common idea among EMC specialists is that excessive shielding is an indication of inadequate attention being paid to other aspects of EMC design and that it is therefore an admission of defeat [2, 3]. Circuits must be designed to minimize emissions and maximize their immunity to interference. However, in practice, is difficult to be sure that an equipment will not experience excessive interference either as a result of unexpected circumstances (such as accidental changing of static or dynamic operating regime of some electronic components or circuits), or due to the negligence of others. Designing a good shield therefore provides a means of controlling interference which is under the designer's control and is relatively immune to external factors.

This paper covers some aspects of the design optimization, from the EMC (and TEMPEST) point of view with application to a shielding box for a portable computer. TEMPEST is usually known as a code name referring to theoretical and practical investigations of electromagnetic compromising emanations which can be regarded as unintentional intelligence-bearing signals which, if intercepted or analyzed, may disclose the information transmitted, received, handled or processed by any suitable equipment.

The TEMPEST aspect of shielding is related to the TEMPEST problem, which is generally referred to the problem to make impossible the information recovery from the electromagnetic emanations of a given device, by all technical means [4]. In fact, the physical mechanisms and phenomena implied by EMC and/or TEMPEST protection of equipments are, practically, the same, the major difference consisting, mainly, in the applicable standards assigned to each of the two domains.

Materials used for enclosure are essential in shielding process. Metallic materials can supply excellent shielding. The traditional approach for EMI shielding relies on the use of conventional metallic shields in the form of bulk sheets or meshes. However, this imposes weight penalties. New materials including intrinsic conductive polymers, amorphous metals and intercalated graphites, powders or fibers in filled polymer composites have replaced metals for various shielding applications in the electronic industry.

There are two major electromagnetic mechanism implied in shielding process: reflection from material surface and absorption in the material volume. Electromagnetic waves incident on the material surface has two type of loss. Part of the wave is reflected (reflection loss) and the other part of the wave is transmitted and attenuated by the material (transmission loss). The effectiveness of the shield is determined by the combined effect of the loss by reflection and loss by absorption.

When the impedance of the wave in free space, η_1, is different from the impedance of the electromagnetic wave, η_2, in the shield material, reflection of electromagnetic waves occurs at the interface. The fenomenon is a function of conductivity (σ), permittivity (ε), magnetic

permeability (μ), and frequency and is independent of the thickness of the material.

Electromagnetic waves penetrating in the shield material are attenuated by the material. The electromagnetic energy is transformed in thermal energy. Shields made of electromagnetic absorbing materials attenuate the electromagnetic waves and substantially solve EMI problems. The absorption loss does not depend on the wave impedance of the incident field and thus is not related to the near - or far-field conditions. The shield's effectiveness depends on shield geometry, type of field component (electric or magnetic) being attenuated, angles of incidence, frequency and polarization. The materials used as electromagnetic absorbers can be classified in:

- materials with high dielectric constant which absorb the electric field component energy and

convert it into thermal energy (e.g. carbon particles, $BaTiO_3$)

- materials with high permeability which absorb the magnetic field component energy and convert it into thermal energy (i.e. ferrite materials, Fe_3O_4)

Besides EMI suppression electromagnetic absorbing materials have applications in many fields (i.e. microwave noise control, microwave antenna patterning, radar camouflage and stealth technology)

The shielding effectiveness (SE) factor may be expressed as the ratio of the transmitted field magnitude to the incident field magnitude [5]. The shielding effectiveness figure may be expressed as:

$$SE = 20 \log\left(\frac{E_0}{E_s}\right), \quad \langle dB \rangle \tag{1}$$

where: E_0 - the electric field intensity in the absence of the screen E_s - the electric field intensity in the presence of the screen

Magnetic shielding effectiveness is similarly defined:

$$SE = 20 \log\left(\frac{H_0}{H_s}\right), \quad \langle dB \rangle \tag{1'}$$

where: H_0 - the magnetic field intensity in the absence of the screen; H_s - the magnetic field intensity in the presence of the screen

There are several mechanisms which make a shield less than perfect [4, 7]:

a.   penetration through the shield wall
b.   coupling through wires penetrating the shield
c.   penetration through apertures

For a highly conducting shield, mechanism *(a)* is not significant when *(b)* and/or *(c)* are present, except at low-frequencies and for magnetic fields. Mechanism *(b)* is significant but is less dependent on shield design than on filtering and bonding at the entry point. Mechanism *(c)* is significant and strongly influenced by shield design.
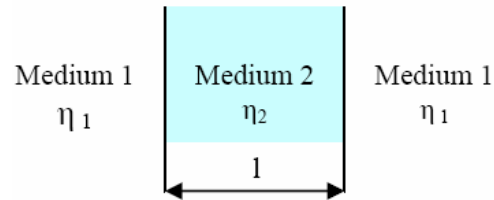

Fig. 1. General representation of an electromagnetic shield. (η_1, η_2 – impedance of medium 1 and 2).

The electronic equipment can be effectively shielded by the use of a conductive barrier placed in between the source of electromagnetic waves and the equipment to be shielded, as shown in Fig. 1.

2. Computing the electromagnetic field propagating through a material

Considering (Fig. 1) a shield material (medium 2 with impedance η_2) placed in air (medium 1 with impedance η_1), the permeability (μ), permittivity (ε) and conductivity (σ) can be taken to be approximately the same of the free space: $\mu = \mu_o$, $\varepsilon = \varepsilon_o$, $\rho = 0$ and J = 0 (the free current density) [6]. For a perfect conductor $\sigma \rightarrow \infty$ but ε and μ are finite and all time-varying fields are zero. For a lossless medium $\sigma = 0$ (perfect dielectric) but ε and μ are finite. For a good conductor conduction current > displacement current, ($\sigma \gg \omega\varepsilon$) and for a good dielectric displacement current > conduction current ($\omega\varepsilon \gg \sigma$)

For a material of given characteristics (namely ε_r, μ_r, σ), we developed a representation of the field propagating through it, taking into account the following initial assumptions [8]:

- region free of charge or current: $\overline{J} = \overline{M} = 0$
- the medium (ε_r, μ_r) will be assumed to be:
- linear (field-independent)
- isotropic (direction independent)
- non-dispersive (frequency independent)

The one-dimensional scalar wave equation is given by:

$$\frac{\partial^2 E_z}{\partial t^2} = c^2 \frac{\partial^2 E_z}{\partial x^2} \tag{2}$$

where: E_z – electric field intensity (z component, TEM mode); t – time; x – space (direction of propagation, Ox)

Relation (2) shows that a z-directed electric field will propagate along the x-axis in time, with a velocity of c. As in any wave equation, the solutions of equation (2), which is a second-order partial differential equation (PDE), will have two linearly independent solutions:

$$u(x,t) = F(x + ct) + G(x - ct) \tag{3}$$

where: $u(x,t) = F(x+ct) + G(x-ct)$ is a solution of the 1D wave equation regardless of the choice of F and G.

Based on above mentioned assumptions and facts we modeled the propagation of the field (one-dimensional case), for an arbitrary material, characterized by different values of dielectric permittivity, ε_r, and conductivity, σ. The Matlab (.*m* file), used for the simulations whose results are displayed above (Fig. 1), implements the finite-difference time-domain solution of Maxwell's curl equations:

$$\nabla \times \overline{e}(\overline{r},t) = -\frac{\partial}{\partial t} b(\overline{r},t) \qquad (4)$$

$$\nabla \times \overline{h}(\overline{r},t) = \overline{j}(\overline{r},t) + \frac{\partial}{\partial t} \overline{d}(\overline{r},t) \qquad (5)$$

where: e – electric field intensity,
b – magnetic field induction,
h – magnetic field intensity,
d – electric displacement,
r – position vector,
t – time.

The implementation is done over a one-dimensional space lattice comprised of uniform grid cells. To illustrate the algorithm, a sinusoidal wave (1GHz frequency) propagating in a non-permeable lossy medium was used and the simplified finite difference system for non-magnetic media was implemented. The grid resolution ($\partial x = 1.5\ cm$) was chosen to provide 20 samples per wavelength.

In Figs. 2 and 3 the simulated electric field of an electromagnetic wave propagating in different arbitrary materials is depicted. In Fig. 2 materials are characterized by $\sigma = 10^{-2}\ S.m^{-1}$ for relative dielectric constant values of $\varepsilon_r = 1$ and $\varepsilon_r = 10$. For Fig. 3 materials are characterized by $\sigma = 10^{-1}\ S.m^{-1}$ for the relative dielectric constant values of $\varepsilon_r = 1$ and $\varepsilon_r = 10$.
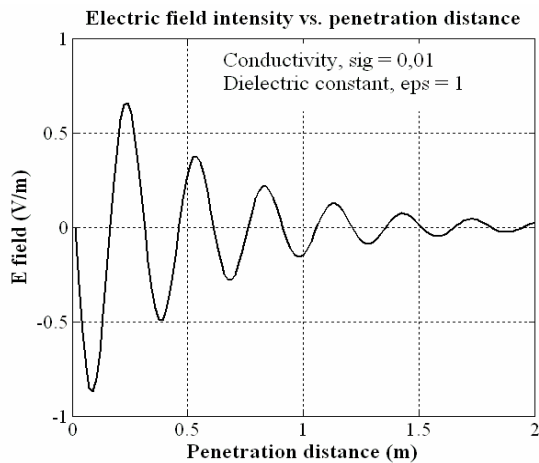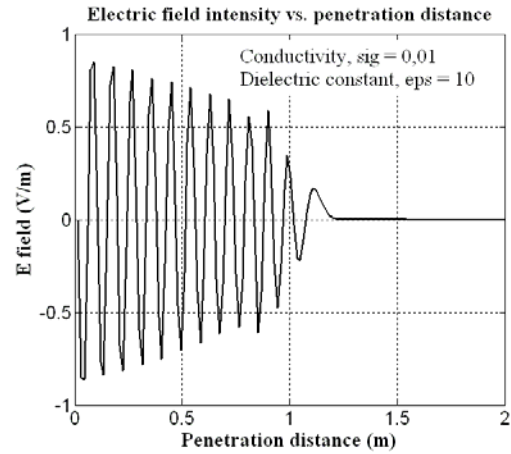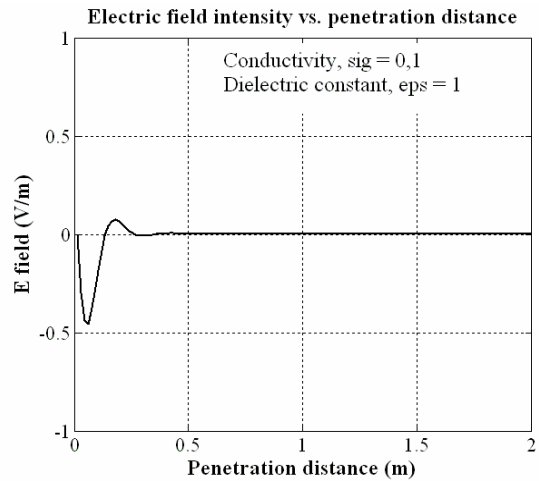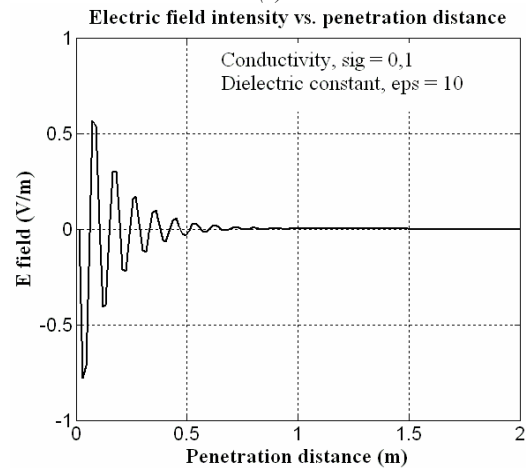

(b)

Fig. 2. Electric field component propagating in two different materials; the materials are characterized by $\varepsilon_r = 1$ (Fig. 2 (a)), respectively $\varepsilon_r = 10$ (Fig. 2 (b)) and $\sigma = 10^{-2}\ S.m^{-1}$.

(a)

(b)

Fig. 3. Electric field component propagating trough two different materials; the materials are characterized by $\varepsilon_r = 1$ (Fig.3. a), respectively $\varepsilon_r = 10$ (Fig.3. b) and $\sigma = 10^{-1}\ S.m^{-1}$.

(a)

It can be seen from Figs. 2 and 3 that the increasing dielectric constant value results in a decreasing of the skin depth in the material. A similar effect is also observed in the case of the increase of the material conductivity.

These facts can be explained taking into account the expression of the skin depth, $\delta_{\varepsilon_r,\sigma}$:

$$\delta_{\varepsilon_r,\sigma} = \frac{1}{2\pi f \sqrt{\dfrac{\mu_0 \mu_r \varepsilon_0}{2} \varepsilon_r \left(1 + \sqrt{1 + \left(\dfrac{\sigma}{2\pi f \varepsilon_0 \varepsilon_r}\right)^2}\right)}} \qquad (6)$$

where: $\delta_{\varepsilon_r,\sigma}$ - skin depth,

f   - operating frequency (1 GHz),

μ_r - permeability of the material ($\mu_r = 1$, assuming a non-magnetic material),

σ - electric conductivity of the material,

ε_r - relative dielectric constant of the material,

μ_0 - $\mu_0 = 4\pi 10^{-7}$ H/m- free space permeability,

ε_0 - 8.85416×10^{-12} F/m - free space permittivity.

Skin depth variation with ε_r, for some particular values of σ, is shown in Fig. 4 and a 3D representation of the skin depth variation with conductivity and dielectric constant is presented in Fig. 5. The last representation has the advantage to show the dependence of δ on both ε_r and σ, simultaneously.
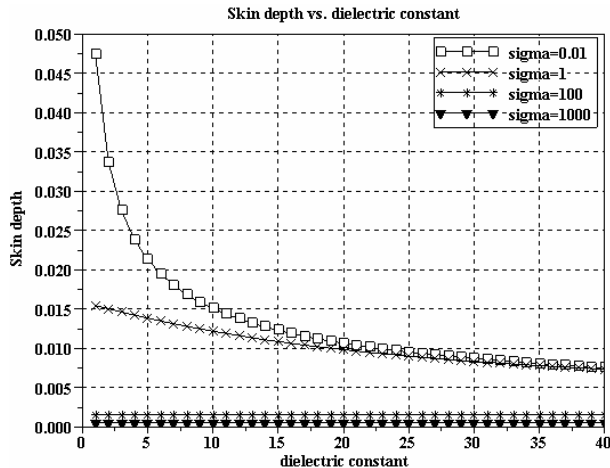

Fig. 4. *The skin depth as a function of the dielectric constant, for several values of electrical conductivity.*

The increasing of the relative permittivity has the effect of decreasing the skin depth, as resulted from Figs. 4 and 5, and as a direct consequence, the attenuation of the electric field component in the material is higher.
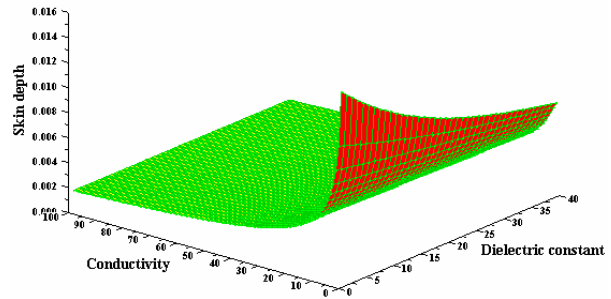

Fig. 5. *The skin depth as a function of the dielectric constant and electrical conductivity.*

This is equivalent to the effect of increasing the frequency, *f*, of the electromagnetic waves (or decreasing of the wavelength of the oscillation propagating in the material).

2. Numerical modeling of an electromagnetic shield box as a multimode cavity

The main purpose of the work presented in this paper, was to estimate the shielding performance of a metallic box designed to protect, both TEMPEST and EMC, a portable computer (length= 362 mm, height=73.7mm, width=317 mm).

The simulation was carried out using a derivation of FDTD general method in order to make an evaluation of some really occurring situations. This includes the existence of both, accidental discontinuities (mainly rectangular or quasi-rectangular slots - which can be eliminated by using a of proper technology) and unavoidable discontinuities (mainly holes) with various destinations (technological, heating / ventilation, etc.) [9, 10].

Each one of the above mentioned discontinuities has some influence on the magnitude and directional characteristics of the parasitic (unwanted) radiated field. This influence has been evaluated by simulation.

The simulation was carried out according to the general design procedure of an electric shield, which involves, in general, a compromise between the necessary (i.e. unavoidable) apertures in the shield and the requested shield radiation level. The shielding box, used for simulation purposes, has the shape and dimensions as in Fig. 6.

The radiation level is imposed by various standards - in our case we used the limits from FCC Regulations, part 15, subpart J, (Computing Devices). According to this standard, there are two classes of devices, each one characterized by different level of the radiated electric field intensity: class A (intended for commercial, industrial and business use) and class B, for home /consumer use.

Some of the most important simulation results are presented in Figs. 7, 8 and 9.
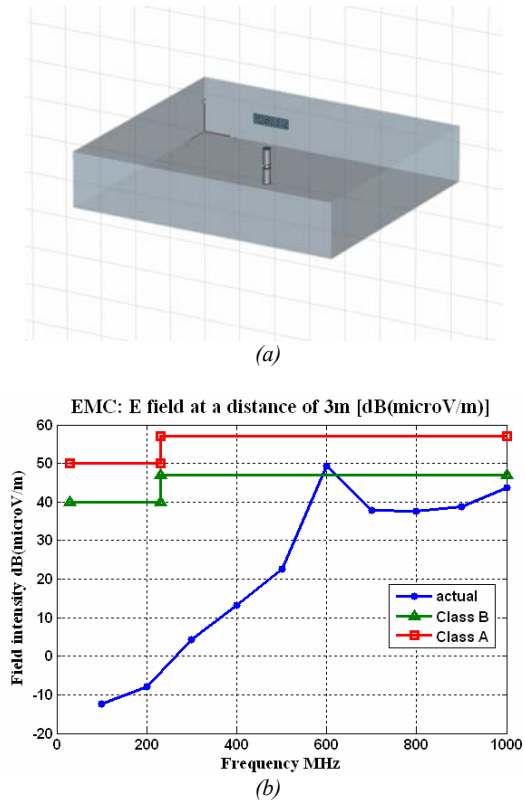

(a)

(b)

Fig. 7. (a) Shielding box with 33 holes (2 mm diameter each, on three rows) unprotected from EMC and TEMPEST; (b) Radiated field intensity variation with frequency diagram, for shielding box from Fig.7a (the limits marked class A and class B on the E filed levels plots are according to the FCC regulations, part 15, subpart J, Computing Devices [11]).
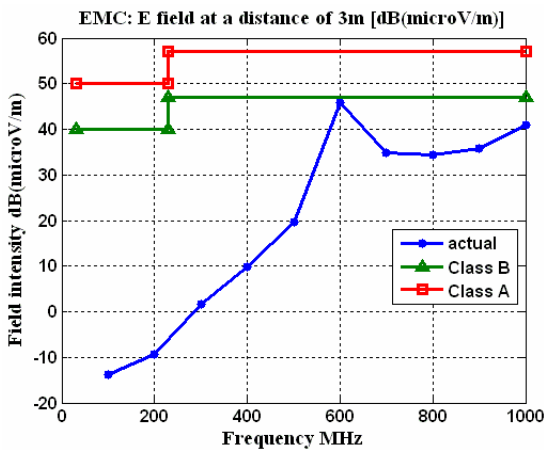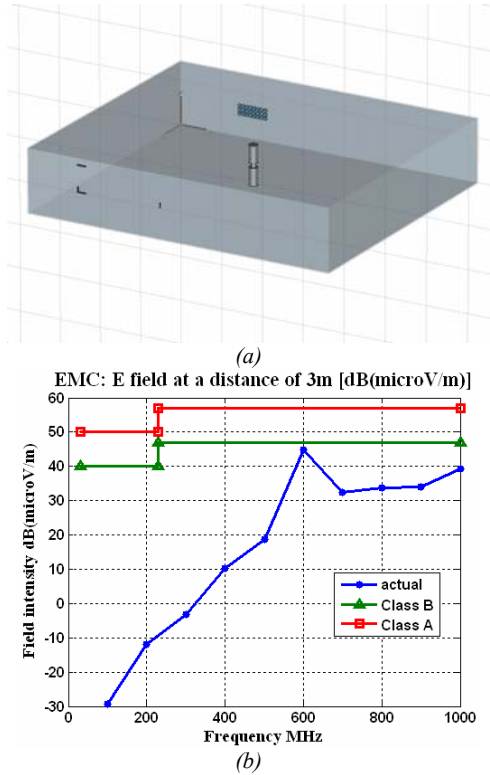

Fig. 8. Field intensity variation with frequency for a shielding box with 28 holes (2 mm diameter each, on three rows) unprotected from EMC and TEMPEST. The limits marked class A and class B on the E filed levels plots are according to the FCC regulations, part 15, subpart J, Computing Devices [11] .

(a)

(b)

Fig. 9. (a) Shielding box with 24 holes (2 mm diameter each, on three rows, one slot of 5 mm and an assembly of three slots mimicking an non- perfect DVD contour slot, unprotected from EMC and TEMPEST; (b) Field intensity variation with frequency for shielding box from Fig. 9 a (the limits marked class A and class B on the E filed levels plots are according to the FCC regulations, part 15, subpart J, Computing Devices [11]).

As one can see from Fig. 7, for the ventilation assembly of 33 holes, the intensity of radiated electric field has a greater value than the class B limits. Reducing the number of holes to 28, the intensity of the radiated electric field is below class B limits, according to the already mentioned standard (Fig. 8). However, the shielding box must have some accesses for the optical unit (i.e. CD-DVD reader/writer), This access was designed and realized to be protected from the TEMPEST and EMC point of view. In practice, in some cases this protection is not well realized; a particular case is modeled by the assembly of three slots, as shown in Fig. 9 (a). If the slot dimensions are less than a given value, which can be determined by a trial method in the simulation procedure, the electric field level is below the class A and class B limits, as can be seen in the plot of the field intensity variation with the frequency in the all 100 – 1000 MHz interval. (Fig. 9 (b))

In all cases from Figs. 7 (b), 8 (b) and 9 (b) the existence of a resonance located around 600 MHz is obvious, resulting from variation with frequency of the electric field intensity radiated by the shielding box . This resonance (the lowest in frequency) is the fundamental resonance of the shielding box, defined in Fig. 6. It confirms the shielding box behavior as a microwave multimode cavity. Slight variation of the resonance frequency is produced by different coupling of the cavity

(shielding box) to the external environment. Changing the coupling (i.e. the number and shape of holes and slots) as in Figs. 7, 8 and 9, the reactance coupling is modified with effects on frequency resonance of the shielding box and also on intensity of radiated electric field.

The radiation diagram of the shielding box for three frequencies: 500 MHz, 600 MHz and 900 MHz is shown in Figs. 10, 11 and 12 for the case of the box from Fig. 9 (a).
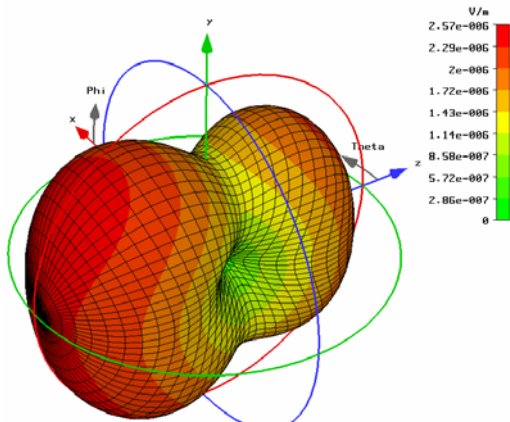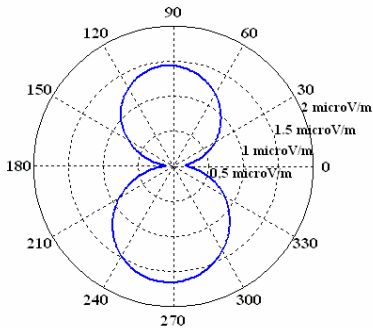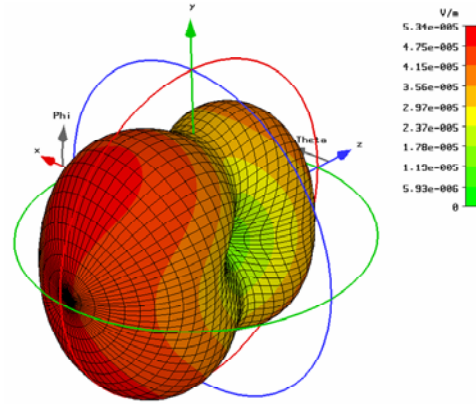

(a)

Directivity diagram in the vertical plane

(b)
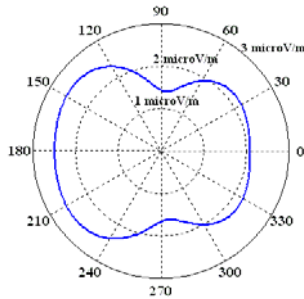
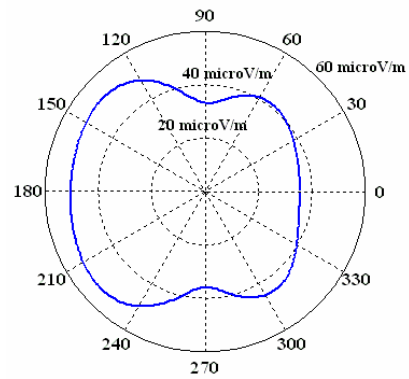**Directivity diagram in the horizontal plane**

(c)

Fig. 10. *Radiation pattern of the shielding box, for the case shown in fig. 9.a. (i.e. the box has 24 holes, 2 mm diameter each, one slot of 5 mm and an assembly of three slots mimicking an non- perfect DVD contour slot, EMC and TEMPEST unprotected) for f = 500 MHz, where f is the frequency of the electric field wave. a) the 3D radiation pattern; b) 2D vertical radiation pattern; c) the 2D horizontal radiation pattern. All the patterns correspond, spatially, to the situation when the shielding box is seen with the face containing the holes.*
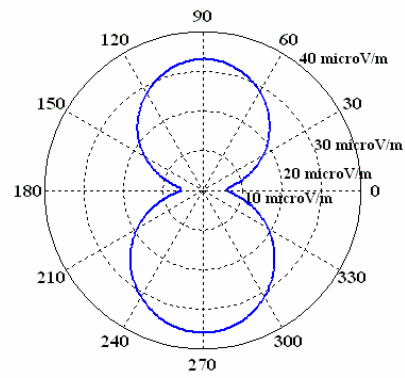

(a)

Directivity diagram in the vertical plane
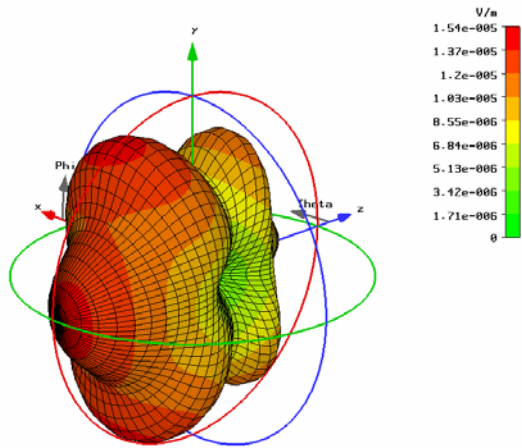

(b)

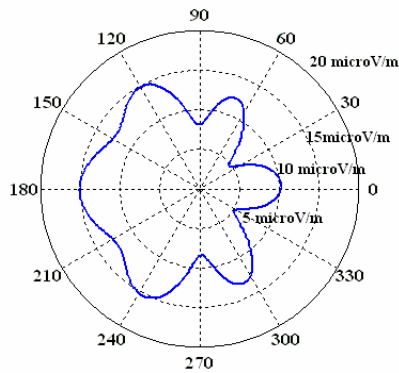**Directivity diagram in the horizontal plane**

(c)

Fig. 11. *Radiation patterns of the shielding box, for the case shown in Fig. 9 a (i.e. the box has 24 holes, 2 mm diameter each, one slot of 5 mm and an assembly of three slots mimicking an non- perfect DVD contour slot, unprotected from EMC and TEMPEST point of view) for f = 600 MHz where f is the frequency of the electric field wave. a) the 3D radiation pattern; b) 2D vertical radiation pattern; c) the 2D horizontal radiation pattern. All the patterns correspond, spatially, to the situation when the shielding box is seen with the face containing the holes.*

(a)

(b)

(c)

Fig. 12. Radiation pattern of the shielding box, for the case shown in fig. 9 a (i.e. the box has 24 holes, 2 mm diameter each, one slot of 5 mm and an assembly of three slots mimicking an non- perfect DVD contour slot, unprotected from EMC and TEMPEST point of view) for f = 900 MHz, where f is the frequency of the electric field wave. a) the 3D radiation pattern; b) 2D vertical radiation pattern; c) the 2D horizontal radiation pattern. All the patterns correspond, spatially, to the situation when the shielding box is seen with the face containing the holes.
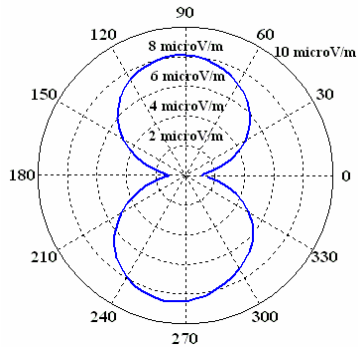
It can be seen, from Fig. 10, that the radiated field is maximum on the face containing the holes, showing that the contribution of these ones is more significant than of the slots' one, situated on the opposite face (see Fig. 9 (a)).

The hole behavior is similar to an antenna array one, the holes assembly being the equivalent to an array of elementary radiators of circular shape. As a consequence, one can notice some issues specific to the arrays' field:

▪ scan of the main beam of the radiation pattern due to the frequency variation (from 140°, for $f = 500 MHz$ - see Fig. 10 (b) - the 2D vertical pattern, up to 158°, for $f = 900 MHz$ - see Fig. 12 (b) - the 2D vertical pattern);

▪ grating lobes apparition (see Fig. 12 (b) - the 2D vertical pattern),

▪ variation of the angular width (both in vertical and horizontal planes, (see Figs. 10, 11 and 12 - the 2D patterns).

3. Conclusions

Some aspects [of] the design optimization including materials considerations, from the EMC and TEMPEST point of view, with application to a shield for a portable computer, was presented in this paper.

The selection of the shielding barrier material is essential in the shielding process to meet electromagnetic compatibility requirements.

Simulations were carried out in order to have an evaluation of shielding effectiveness for a shielding box, including the existence of both some accidental discontinuities (mainly rectangular, or quasi-rectangular slots - which can be eliminated by use of proper technology) but also the existence of unavoidable discontinuities (mainly holes) having various destinations (technological, heating / ventilation etc.).

The shielding enclosure has a resonance frequency determined by the shape, dimensions and coupling with the external environment. This value is important to be determined, in conjunction with the frequency of the fields existing and propagating into the electronic equipment shielded, in order to prevent the radiated field. The simulation reveals a radiating behavior of the shielding box with the electronic equipment when slots and holes are present in the shield.

The level of the radiating electromagnetic field can be reduced, in order to be maintained below the limits from both EMC and TEMPEST standards, by proper use of radiofrequency and microwave simulation techniques and by a suitable design and technology.

References

[1] S. Pennesi, Proc. 2005 Intern. Symposium on Electromagnetic Compatibility **3**, 777 (2003).
[2] W. A. Radasky, Proc. Intern. Symposium on Electromagnetic Compatibility **2**, 531 (2003).

[3] M. P. Robinson, Proc. IEEE Colloq. on Achieving
    Electromagnetic Compatibility, 3/1, 2005.
[4] M. G. Kuhn, Technical Report no. 577, University of
    Cambridge, Computer Laboratory, Cambrige,U.K.,
    2003.
[5] D. G. Svetanoff, Proc.IEEE Intern. Symposium on
    Electromagnetic Compatibility **2**, 1016 (1999).
[6] M. Feliziani, Proc.IEEE Intern. Symposium on
    Electromagnetic Compatibility **1**, 167 (2001).
[7] V. M. Primiani, Proc. IEEE Intern. Symposium on
    Electromagnetic Compatibility, 1, 2007.

[8] M. Feliziani, Proc. IEEE Trans. on Mag. **36**(4), 848
    (2000).
[9] R. Araneo, Proc IEEE Intern. Symposium on
    Electromagnetic Compatibility **2**, 755 (2000).
[10] A. R. Attari, Proc. IEEE Antennas and Propagation
    Society Intern. Symposium **3**, 302 (2002).
[11] Federal Communications Commission, FCC
    regulations, part 15, subpart J, Computing Devices,
    Federal Register, Washington, DC 20554, USA,
    2008.

_____
[*]Corresponding author: ioachim@infim.ro